Earth Syst. Dynam. Discuss., https://doi.org/10.5194/esd-2018-14
Manuscript under review for journal Earth Syst. Dynam.
Discussion started: 23 March 2018

Earth System Dynamics
Discussions
Open Access
EGU

A Theory of Pleistocene Glacial Rhythmicity

Mikhail Y. Verbitsky[1*], *Michel Crucifix*[2], *and Dmitry M. Volobuev*[1]

[1]The Central Astronomical Observatory of the Russian Academy of Sciences at Pulkovo, Saint Petersburg, Russia
[2]Georges Lemaître Centre for Earth and Climate Research, Earth and Life Institute, Université catholique de Louvain, Louvain-la-Neuve, Belgium
*e-mail: verbitskys@gmail.com

Abstract. Variations of Northern Hemisphere ice volume over the past 3 million years have been described in numerous studies and well documented. These studies depict the mid-Pleistocene transition from 40-ky oscillations of global ice to predominantly 100-ky oscillations around 1 million years ago. It is generally accepted to attribute the 40-ky period to astronomical forcing, and to attribute the transition to the 100-ky mode to a phenomenon caused by a slow trend which, around the mid-Pleistocene, enabled the manifestation of non-linear processes. However, both the physical nature of this non-linearity, and its interpretation in terms of dynamical systems theory, are debated. Here, we show that ice sheet physics, coupled with a linear ocean feedback, conceal enough dynamics to satisfactorily explain the system response over the full Pleistocene. There is no need, a priori, to call for a non-linear response of the carbon cycle. Without astronomical forcing, the obtained dynamical system evolves to equilibrium. When it is astronomically forced, then, depending on the values of parameters involved, the system is capable of producing different modes of non-linearity and consequently - different periods of rhythmicity. The crucial factor that defines a specific mode of system response is the relative intensity of glaciation and ocean feedbacks. To measure this factor, we introduce a dimensionless variability number *V*. When ocean positive feedback is weak (*V*~0), the system exhibits fluctuations with dominating periods of about 40 ky which is in fact a combination of doubled precession period and (to smaller extent) obliquity period. When ocean positive feedback increases (*V*~0.75), the system evolves with a roughly 100-ky period due to doubled obliquity period. If ocean positive feedback increases further (*V*~0.95), the system produces fluctuations of about 400 ky. When *V*-number is gradually increased from its low early Pleistocene values to its late Pleistocene value of *V*~0.75, the system reproduces mid-Pleistocene transition from mostly 40-ky fluctuations to 100-ky-period rhythmicity. Since *V*- number is a combination of multiple parameters, it implies that multiple scenarios are possible to account for the mid-Pleistocene transition. Thus, our theory is capable to explain all major features of the Pleistocene climate such as mostly 40-ky fluctuations of the early Pleistocene, a transition from an early Pleistocene type of non-linear regime to a late Pleistocene type of non-linear regime, and 100-ky fluctuations of the late Pleistocene.

When the dynamical climate system is expanded to include Antarctic glaciation, it becomes apparent that ocean positive feedback (or its absence) plays a crucial role in the Southern Hemisphere as well. While Northern Hemisphere insolation impact is amplified by the ocean and eventually affects Antarctic climate, the Antarctic ice sheet area of glaciation is limited by the area of the Antarctic continent, and therefore it cannot engage strong positive feedback from the ocean. This may serve as a plausible explanation of the synchronous response of the Northern and Southern Hemispheres to Northern Hemisphere insolation variations.

Given that the *V*- number is dimensionless, we consider that this model could be used as a framework to investigate other physics which may possibly be involved in producing ice ages. In such a case, the equation currently representing ocean temperature would describe some other climate component of interest, and as long as this component is capable of producing an appropriate *V*-number, it may perhaps be considered a feasible candidate.

1. Introduction

Existing empirical records provide significant evidence that glacial oscillations during the last 3 million years experienced major change of their modes of rhythmicity, switching from predominately near-40 ky period fluctuations of early Pleistocene to about-100 ky oscillations in the late Pleistocene. During the last 50 years,

Earth Syst. Dynam. Discuss., https://doi.org/10.5194/esd-2018-14
Manuscript under review for journal Earth Syst. Dynam.
Discussion started: 23 March 2018

Earth System Dynamics
Discussions
Open Access
EGU

considerable efforts of the scientific community have been directed to the explanation of these phenomena. A systematic review of the last century's work was presented by Barry Saltzman (2002) in his last book. An insightful overview of more recent efforts can be found, for example, in (Clark et al., 2006, Tziperman, et al., 2006, Crucifix, 2013, Mitsui and Aihara, 2014, Paillard, 2015, Ashwin and Ditlevsen, 2015). As of today, it is widely acknowledged that 23-ky and 40-ky fluctuations of Pleistocene global ice volume represent a climate system response to astronomical forcing on precession and obliquity frequency bands. At the same time, the causes of major late Pleistocene 100-ky oscillations as well as the explanation of the physics which led to the transition from the 40-ky period to the 100-ky period remain unsettled.

In some previous work (Saltzman and Verbitsky 1992, 1993a, b; 1994a, b) we attempted to explain the nature of Pleistocene ice ages using a dynamical global climate model describing evolution of global ice mass, bedrock depression, atmospheric carbon dioxide concentration, and ocean temperature. The central piece of this model was the ice-carbon dioxide oscillator, which produced 100-ky cycles. As a justification, we considered the evolution of the global climate system on a phase plane using empirical data of global ice volume against records of carbon dioxide concentration (Saltzman and Verbitsky, 1994a). This phase diagram supported our assumption that carbon dioxide leads ice volume changes. Other authors have advanced similar proposals. For example, Paillard and Parrenin (2004) present a simple model of ice-sheet-ocean and carbon-cycle dynamics. The non-linear terms, which are necessary to generate the mid-Pleistocene transition as well as the 100-ka mode, are located in the ocean and carbon cycle equations. However, this explanation needs to be challenged. First, a detailed discussion of the timing of CO_2 and the benthic isotopic record leaves open the possibility that at the time scale of the glacial-interglacial cycle the CO_2 simply acts as a feedback on ice volume (Ruddiman 2006), even if it is also observed that the dynamics of the deglaciation are complex and that CO_2 changes can go through fairly abrupt dynamics (Ganopolski and Roche, 2009). On the other hand, other potential elements in the Earth System could generate non-linearities yielding 100-ky cycles: Ashkenazy and Tziperman (2004) proposed a "sea-ice switch", Imbrie, *et al* (2011) interpret the non-linear terms of their models as a representation of ice sheet instability; Ellis and Palmer (2016) resort to a dust albedo feedback, while Omta et al. (2016) invoke an instability of the carbonate cycle. There is a plethora of possible mechanisms, but the mathematical expression of these various mechanisms is scarcely firmly constrained. The physical cause of ice age cycles remain, for that reason, largely contentious. In parallel, simulations based on models with more physically and geographically explicit models, such as models of intermediate complexity of Verbitsky and Chalikov (1986), Chalikov and Verbitsky (1990), Ganopolski et al (2010), and the higher-resolution ice-sheet-climate model of Abe-Ouchi *et al* (2013), confirm the important role of ice sheet dynamics in shaping the 100-ky cycle.

In this paper, our aim is to approach this question from a different perspective. The approach proposed here is both reductionist – we rely on laws of thermo-hydrodynamics – and parsimonious: we intend to explain the phenomenon of interest (the apparition and repetition of ice ages cycles) with a minimal set of assumptions. We limit ourselves to just two components that, without a doubt, should be part of any ice-age story: ice sheets and the ocean. We will demonstrate that astronomical forcing may prompt different modes of glacial rhythmicity (including periods of 23-ky, 40-ky, 100-ky, and 400-ky) of a global climate system that, without astronomical forcing, does not oscillate. For this purpose, we will derive a simple dynamical system using scaled equations of ice sheet thermodynamics and combining them with an equation describing the evolution of ocean temperature. Without astronomical forcing, this system evolves to equilibrium. When it is astronomically forced, it may produce different modes of rhythmicity.

We will show that the critical system property that defines system response to astronomical forcing is a specific balance between intensities of positive and negative feedbacks involved. We will evaluate this balance with a

Earth Syst. Dynam. Discuss., https://doi.org/10.5194/esd-2018-14
Manuscript under review for journal Earth Syst. Dynam.
Discussion started: 23 March 2018

Earth System Dynamics Discussions

variability number (*V*-number), a dimensionless combination of eight model parameters, measuring relative intensity of ocean and glaciation feedbacks. We will demonstrate that, depending on the *V*-number, the mechanism of non-linear amplification of the astronomical forcing will produce different results. We will also show that the intensity of ocean feedback may be a critical factor in explaining the synchronous response of the Northern and Southern Hemispheres to Northern Hemisphere insolation variations.

Accordingly, our paper is organized as follows. First we will derive simple equations representing continental glaciation and test their parameters using sensitivity experiments with a three-dimensional model of the Antarctic ice sheet. We will then combine ice-sheet and ocean equations into a global climate dynamical system and analyze its properties. We will inspect all feedbacks present in the system and suggest a dimensionless criterion (*V*-number) which measures their relative intensity. We will then model our system response to astronomical forcing for different *V*-numbers to reproduce early- and late-Pleistocene modes of glacial rhythmicity as well as the mid-Pleistocene transition. Finally, we will expand our system to include the Antarctic glaciation.

2. Scaling model of the continental glaciation

As we have explained in the introduction, our ambition is to follow a parsimonious approach but rely on reductionism. To achieve this agenda, we will apply scaling analysis to conservation equations. Indeed, scaling analysis provides simple mathematical statements which do not compromise the integrity of physical laws. Accordingly, we begin with the mass, momentum, and heat conservation equations for a thin layer of homogeneous non-Newtonian ice:

$$\frac{\partial u}{\partial x}+\frac{\partial w}{\partial z}=0 \tag{1}$$

$$-\frac{\partial p}{\partial x}+\frac{\partial \sigma_{xz}}{\partial z}=0 \tag{2}$$

$$-\frac{\partial p}{\partial z}-\rho g=0 \tag{3}$$

$$\frac{dT}{dt}=k\left(\frac{\partial^2 T}{\partial x^2}+\frac{\partial^2 T}{\partial z^2}\right)+q/(\rho c_i) \tag{4}$$

Here x and z are the horizontal and vertical coordinates, p is pressure, u and w are the horizontal and vertical velocity components, σ_{xz} is the shear stress, ρ is density, c_i is heat capacity, g is the acceleration of gravity, k is the temperature diffusivity, and q is the heat of internal friction. For typical horizontal and vertical dimensions of ice sheets like Antarctic, Laurentide, or Greenland and for typical ice viscosity, the inertial forces are negligible relative to stress gradients, and motion equations with very high accuracy can be written in a quasi-static form (2) - (3) (Paterson, 1981, Verbitsky and Chalikov, 1986).

Earth Syst. Dynam. Discuss., https://doi.org/10.5194/esd-2018-14
Manuscript under review for journal Earth Syst. Dynam.
Discussion started: 23 March 2018

Earth System Dynamics Discussions Open Access EGU

We will now start the process of scaling equations (1) - (4). We introduce the horizontal scale of the ice sheet L, the scale of its thickness H, and the scale of the vertical velocity $W = a$, where a is the scale of the mass influx (net snow accumulation). From the continuity Eq. (1) and hydrostatic Eq. (3) we obtain the scale of the horizontal velocity $U = aL/H$ and the scale of the pressure $P = \rho gH$. From the momentum equation (2) we get the scale of the shear stress $\Sigma = \rho gH^2/L$. The power rheological law $2\mu u_z = \sigma^n$, (where μ is viscosity, u_z is the strain rate, and n is power degree) provides us with an estimate $\mu U = (\rho g)^n H^{2n+1} L^{-n}$. Since $U = aL/H$, and $L = S^{1/2}$ where S is the glaciation area, we can finally get the scale of ice thickness (Vialov, 1958):

$$H = \left[\frac{\mu a}{(\rho g)^n}\right]^{\frac{1}{2n+2}} S^{1/4} \tag{5}$$

We start analysis of energy equation (4) with the notion that for typical glaciological systems the Peclet number $Pe = (aH)/k$ is of order 10. This means that advection dominates the heat conservation equation (4), so that an ice-flow trajectory has a near-constant temperature determined by its value on the top surface of the ice sheet. We will now determine the thickness of the bottom boundary layer η where vertical diffusion, kT_{zz}, gains significance and is balanced by the advection of heat uT_x. Using the scale of the horizontal velocity $U = aL/H$ obtained above and assuming that vertical and horizontal temperature gradients are of the same order of magnitude, we have:

$$\eta = (kH/a)^{1/2} = Pe^{-1/2} H \tag{6}$$

Within this boundary layer, the equation (4) can be reduced to:

$$\lambda \frac{\partial^2 T}{\partial z^2} + q = 0 \tag{7}$$

with boundary conditions $T = T_\eta$ at $z = \eta$, *and* $-\lambda T_z = Q$ at $z = 0$. Here $\lambda = k\rho c$ is heat conductivity, and Q is the geothermal heat flux. Thus the scale of the basal temperature θ can be estimated as a sum of three scales:

The scale of the surface temperature effect:

$$\theta_{surface} = T_\eta = T_S - \gamma H \tag{8}$$

Here we account for the fact that T_η is "delivered" from the ice sheet surface and can be estimated as $T_S - \gamma H$, where T_S is the annual mean sea-level temperature, and γ is vertical atmospheric lapse rate.

The scale of the internal friction effect:

$$\theta_{friction} = \frac{q\eta^2}{\lambda} \tag{9}$$

The heat of the internal friction can be estimated as

$$q = \frac{1}{\mu}\Sigma^{n+1} \tag{10}$$

Earth Syst. Dynam. Discuss., https://doi.org/10.5194/esd-2018-14
Manuscript under review for journal Earth Syst. Dynam.
Discussion started: 23 March 2018

Earth System Dynamics Discussions Open Access EGU

Since $\Sigma = \rho g H^2/L$, H is described by (5), and $S^{1/4}=L^{1/2}$, then

$$q = \rho g a \tag{11}$$

Accounting for (6), the scale of the internal friction effect finally takes form:

$$\theta_{friction} = \frac{\rho g k H}{\lambda} \tag{12}$$

The scale of the geothermal heat flux effect:

$$\theta_{geo} = \frac{Q\eta}{\lambda} \tag{13}$$

It can be seen now that the basal temperature θ is a function of ice thickness H, and because of (5), it is a function of snow precipitation intensity a and of viscosity μ. Since viscosity is temperature dependent, basal temperature is a function of ice temperature T. It is also function of climatic temperature T_S and ice sheet area S. Differentiating equations (8), (12), and (13) along these variables provides us with estimates of basal temperature sensitivity to changing precipitations $\Delta\theta_a$, climatic temperature, $\Delta\theta_T$, and glaciation area $\Delta\theta_S$:

$$\Delta\theta = \Delta\theta_a + \Delta\theta_T + \Delta\theta_S =$$
$$= \frac{\partial(\theta_{surface} + \theta_{fric} + \theta_{geo})}{\partial a}\bigg|^* da + \frac{\partial(\theta_{surface} + \theta_{fric} + \theta_{geo})}{\partial T}\bigg|^* dT + \frac{\partial(\theta_{surface} + \theta_{fric} + \theta_{geo})}{\partial S}\bigg|^* dS$$

$$\Delta\theta_a = \left[-\frac{\gamma H}{2n+2} + \frac{\rho g k H}{(2n+2)\lambda} - \frac{1+2n}{4+4n}\frac{Q\eta}{\lambda} \right]^* \frac{da}{a^*} \tag{14}$$

$$\Delta\theta_T = \left[\left(1 + \frac{1}{2n+2}\frac{\gamma H \vartheta T_m}{T^2}\right) - \frac{1}{(2n+2)}\frac{\rho g k}{\lambda}\frac{H\vartheta T_m}{T^2} - \frac{1}{2(2n+2)}\frac{Q}{\lambda} Pe^{-1/2}\frac{H\vartheta T_m}{T^2} \right]^* dT \tag{15}$$

$$\Delta\theta_S = \left(-\frac{1}{4}\gamma H + \frac{1}{4}\frac{\rho g k}{\lambda} H + \frac{1}{8}\frac{Q}{\lambda} Pe^{-1/2} H \right)^* \frac{dS}{S^*} \tag{16}$$

Asterisk (*) marks undisturbed values in the following sense: If $y=f(x)$, then $\Delta y=(\partial f/\partial x)^*\Delta x$.

In deriving equations (14) - (16), the temperature dependence of viscosity was adopted from Shumskiy (1975):

$$\mu = \mu_o \exp\left[\vartheta(T_0/T - 1)\right] \tag{17}$$

Earth Syst. Dynam. Discuss., https://doi.org/10.5194/esd-2018-14
Manuscript under review for journal Earth Syst. Dynam.
Discussion started: 23 March 2018

Here $\vartheta = 21.1$, T_m is the ice melting temperature (273.15 K). For simplicity, in (14) - (16) we do not differentiate between T and T_S.

In calculating basal temperature response using the scaled equations (14) - (16), the following physical parameter values have been used (Paterson, 1981, Verbitsky and Chalikov, 1986):

$$\gamma = 6.5\times10^{-3} C/m \qquad H = 2{,}000m$$
$$a = 5\times10^{-9} m/s \qquad n = 3$$
$$k = 10^{-6} m^2/s \qquad \rho = 917kg/m^3$$
$$\lambda = 2W/(m\times K) \qquad g = 9.8m/s^2$$
$$Q = 0.04W/m^2$$

It gives us the following sensitivities of basal temperature to external climatic factors:

$$\Delta\theta_a \approx -5.75\frac{da}{a}(^oC)$$
$$\Delta\theta_T \approx 0.98dT(^oC)$$
$$\Delta\theta_S \approx 0.83\frac{dS}{S}(^oC)$$

It can be seen that when snow rate increases, intensified ice advection has a tendency to reduce the basal temperature ($\Delta\theta_a$ is negative) because it reduces the thickness of the basal boundary layer. Since snow rate usually increases with warmer climate, such snow rate increase may at least partially compensate for a corresponding increase in basal temperature.

We tested equations (14) - (16) using numerical experiments with the three-dimensional Antarctic ice sheet model of Pollard and DeConto (2012a) - see Appendix for details and full references. Though our research will be devoted mostly to northern hemisphere ice sheets like Scandinavian or Laurentide, the Antarctic ice sheet model can be a good analogue because it is governed by the same physics. Besides, temperature and snow precipitation rates for Antarctica are well known unlike those for ancient ice sheets. Table A1of the Appendix shows that the sign and order of magnitude of the basal temperature response to climatic forcing predicted by our scaling estimates are consistent with the results of the 3-D ice-sheet model.

We are now ready to formulate the dynamical model of the Pleistocene climate.

3. Simple dynamical model of the glacial cycles

We will derive dynamical equations for three variables, namely the area of glaciation S, ice sheet basal temperature θ, and ocean temperature ω.

3.1 Area of glaciation

We start with the mass conservation equation integrated over the entire ice sheet surface:

Earth Syst. Dynam. Discuss., https://doi.org/10.5194/esd-2018-14
Manuscript under review for journal Earth Syst. Dynam.
Discussion started: 23 March 2018

Earth System Dynamics Discussions Open Access EGU

$$\frac{d(HS)}{dt} = AS \tag{18}$$

Here A is total snow accumulation minus ablation and calving. According to (5),

$$H = \zeta S^{1/4}, \zeta = \left[\frac{\mu a}{(\rho g)^n}\right]^{\frac{1}{2n+2}}$$

then, assuming ζ=const, equation (18) can be written as

$$\frac{dS}{dt} = \frac{4}{5}\zeta^{-1}S^{3/4}A \tag{19}$$

It is interesting that the fundamental mass balance (19) provides some support to the hypothetical model of Huybers (2009). If we consider the right side of (19) to be the rate of deglaciation, then explicit finite differencing of (19) would give us:

$$S_t = S_{t-1} + \frac{4}{5}\zeta^{-1}S_{t-1}^{3/4}A\Delta t$$

where the rate of deglaciation depends on the dimension S_{t-1} of the previous glaciation . It doesn't imply that ice can "remember" its previous state - equation (19) simply tells us that deglaciation of bigger ice sheets occurs on a bigger area.

We adopt the following parameterization for the total mass balance A appearing in equation (19): $A=A_1-A_2-A_3-A_4$.

Here:

(a) $A_1=a$ is snow accumulation rate;
(b) $A_2= \varepsilon F_S$ is ice ablation rate due to astronomical forcing F_S, the local mid-July insolation at 65°N (Berger and Loutre, 1991);
(c) $A_3=\kappa\omega$ is ice ablation rate representing cumulative effect of the global climate on ice-sheet mass balance. Variable ω, which we are going to call for simplicity the "ocean temperature", is in fact a cumulative proxy of the climate system outside of glacier. Accordingly, any climate induced changes of ice-sheet mass balance are functions of ω. Increased climate temperature (in our system - ocean temperature ω) affects ice-sheet mass balance in several ways:
    - It changes (likely, increases) snow precipitation
    - It intensifies ablation
    - It intensifies ice discharge due to reduced viscosity
    - Corresponding changes in greenhouse gas concentration (CO_2) affect the radiative balance of the atmosphere
(d) $A_4= c\theta$ represents ice discharge due to ice-sheet basal sliding. Variable θ, which for simplicity we are going to call "basal temperature", is in fact a measure of ice sheet intensity of basal sliding. The basal temperature

Earth Syst. Dynam. Discuss., https://doi.org/10.5194/esd-2018-14
Manuscript under review for journal Earth Syst. Dynam.
Discussion started: 23 March 2018

cannot exceed the melting point, but at that point, continual influx of heat due to internal friction, or geothermal heat flux, or heat of sliding can still increase the intensity of basal melting and facilitate sliding. This type of transition from the frozen bed to sliding conditions has been conceptually described by MacAyeal (1993) and further investigated by Payne (1995) and Marshall and Clark (2002) for Laurentide ice sheet.

(e) Parameters ε, κ, and c are sensitivity coefficients;

Accordingly, equation (19) takes the final form:

$$\frac{dS}{dt} = \frac{4}{5}\zeta^{-1}S^{3/4}(a - \varepsilon F_S - \kappa\omega - c\theta) \tag{20}$$

3.2. Basal temperature

Scales (14) - (16) were obtained for the equilibrium state of the ice sheet. We now account for the fact that changes (14) - (16) follow climate change with a time lag equal to a characteristic vertical advection rate H/a:

$$\frac{d\theta}{dt} = \frac{\Delta\theta_a + \Delta\theta_T + \Delta\theta_S - \theta}{H/a} \tag{21}$$

We substitute scales (5) and (14) - (16) into (21). We combine $\Delta\theta_a$ and $\Delta\theta_T$ together, assuming that $\Delta\theta_a$ is proportional to $\Delta\theta_T$, and $\Delta\theta_T$ is proportional to ω : $\Delta\theta_a + \Delta\theta_T \sim \alpha\omega$. We replace $\Delta\theta_S \sim \Delta S/S$ of equation (16) with $\Delta\theta_S \sim \beta (S\text{-}S_0)$ where S_0 is a reference glaciation area. Here α and β are sensitivity coefficients. We also modify a like in (20), but without basal sliding because basal sliding is associated with horizontal movements and does not contribute into vertical advection: $A_1\text{-}A_2\text{-}A_3 = a\text{-}\varepsilon F_S\text{-}\kappa\omega$. Thus equation (21) takes the following form:

$$\frac{d\theta}{dt} = \zeta^{-1}S^{-1/4}(a - \varepsilon F_S - \kappa\omega)\{\alpha\omega + \beta[S - S_0] - \theta\} \tag{22}$$

3.3 Ocean temperature

Ocean temperature equation is adopted from Saltzman and Verbitsky (1993a, b):

$$\frac{d\omega}{dt} = \gamma_1 - \gamma_2[S - S_0] - \gamma_3\omega \tag{23}$$

Where γ_1 and γ_3 define its steady state value, $1/\gamma_3$, is response-time constant. It is reasonable to assume here that ω is controlled by polar ice sheets and associated ice shelves ($-\gamma_2[S\text{-}S_0]$, γ_2 being a measure of the strength of such control) but the term $-\gamma_2[S\text{-}S_0]$ may also contain effects of albedo change or other atmospheric feedbacks. Again, what we will call "ocean temperature" (ω) is in fact a cumulative proxy of outside-of-glacier climate, deep ocean being an important component of it. Accordingly, the time scale $1/\gamma_3$ is of order of magnitude of few thousand years to capture the involvement of the deep ocean.

Our three-variable dynamical global climate system then takes its final shape:

Earth Syst. Dynam. Discuss., https://doi.org/10.5194/esd-2018-14
Manuscript under review for journal Earth Syst. Dynam.
Discussion started: 23 March 2018

Earth System Dynamics Discussions Open Access EGU

$$\begin{cases} \dfrac{dS}{dt} = \dfrac{4}{5}\zeta^{-1}S^{3/4}(a - \varepsilon F_S - \kappa\omega - c\theta) & (24) \\ \dfrac{d\theta}{dt} = \zeta^{-1}S^{-1/4}(a - \varepsilon F_S - \kappa\omega)\{\alpha\omega + \beta[S - S_0] - \theta\} & (25) \\ \dfrac{d\omega}{dt} = \gamma_1 - \gamma_2[S - S_0] - \gamma_3\omega & (26) \end{cases}$$

4. Modes of glacial rhythmicity

4.1 Dimensionless measure of glacial rhythmicity: *V*-number.

First, we will inspect feedback loops in equations (24) - (26) as they are portrayed in Fig. 1.

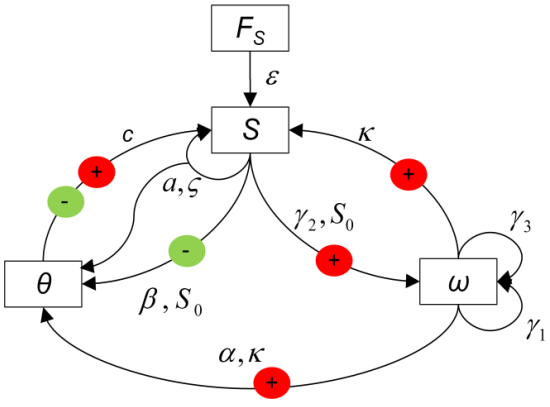

Fig. 1. Dynamical system connections. Red circles mark positive-feedback loops, green circles mark negative-feedback loops.

There are three feedback loops in our system, one negative feedback and two positive feedbacks. Basal temperature θ provides negative feedback to the glaciation area S: When ice sheet grows it increases basal temperature (βS) and creates more favorable conditions for basal sliding which tend to reduce glaciation dimensions ($-c\theta$). When ice retreats, the bottom temperature reduces and tends to preserve glaciation area. There are two positive feedback loops associated with ocean temperature ω: When ice grows it reduces ocean temperature ($-\gamma_2 S$) which in turn increases mass balance on ice sheet surface ($-\kappa\omega$). It also reduces temperature on the ice sheet surface ($\alpha\omega$), this temperature change will propagate to the bottom. Both of these changes will help to build even bigger ice sheet. When ice sheet retreats, ocean temperature rises, and through increased ablation and increased bottom temperature it makes this retreat even faster.

Earth Syst. Dynam. Discuss., https://doi.org/10.5194/esd-2018-14
Manuscript under review for journal Earth Syst. Dynam.
Discussion started: 23 March 2018

Without astronomical forcing, system (24) - (26) evolves to equilibrium (Fig.2).

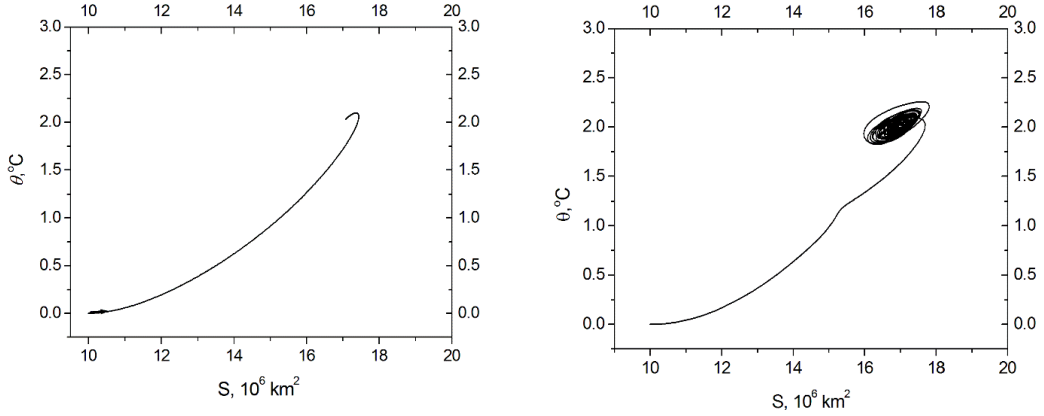

Fig 2. System (24) - (26) evolution without astronomical forcing involved, ε=0 (**left**); the same with very weak forcing, ε=0.01 (**right**)

The results of Figure 2 were obtained with the following values of system parameters:

$\zeta = 1.0(10^{-3/2} km^{1/2})$

$a = 0.065 km/kyr$

$\kappa = 0.005 km/(kyr \times C)$

$c = 0.042 km/(kyr \times C)$

$\alpha = 2.$

$\beta = 2.(^{o}C/10^{6} km^{2})$

$\gamma_1 = 0.^{o}C/kyr$

$\gamma_2 = 0.2^{o}C/(10^{6} km^{2} \times ky)$

$\gamma_3 = 0.25 kyr^{-1}$

$S_0 = 12(10^{6} km^{2})$

For a steady-state solution of Fig.2 (left) ε=0. To test stability of the equilibrium point, we repeated calculations with a weak insolation forcing, ε=0.01. The results, presented in Fig. 2 (right) show that the equilibrium point is stable.

Initial conditions are:

$S(0) = 10.(10^{6} km^{2})$

$\theta(0) = 0.^{o}C$

$\omega(0) = 2.^{o}C$

This steady state solution can be obtained from the system (24) - (26) if we set all derivatives equal to zero:

Earth Syst. Dynam. Discuss., https://doi.org/10.5194/esd-2018-14
Manuscript under review for journal Earth Syst. Dynam.
Discussion started: 23 March 2018

$$0 = \frac{4}{5}\zeta^{-1}S^{3/4}(a - \varepsilon F_S - \kappa\omega - c\theta) \tag{27}$$

$$0 = \zeta^{-1}S^{-1/4}(a - \varepsilon F_S - \kappa\omega)\{\alpha\omega + \beta[S - S_0] - \theta\} \tag{28}$$

$$0 = \gamma_1 - \gamma_2[S - S_0] - \gamma_3\omega \tag{29}$$

Then for ε=0:

$$\langle S\rangle = S_0 + \frac{\frac{a}{c} - \left(\alpha + \frac{\kappa}{c}\right)\frac{\gamma_1}{\gamma_3}}{\beta - \left(\alpha + \frac{\kappa}{c}\right)\frac{\gamma_2}{\gamma_3}} \tag{30}$$

$$\langle\theta\rangle = \frac{a - \kappa\omega}{c} \tag{31}$$

$$\langle\omega\rangle = \frac{\gamma_1 - \gamma_2(\langle S\rangle - S_0)}{\gamma_3} \tag{32}$$

Here $\langle S\rangle$, $\langle\theta\rangle$, and $\langle\omega\rangle$ are steady state solutions of corresponding variables.

It can be seen that without ocean involved (γ_1=γ_2=0, or α=κ=0), the steady-state extent of glaciation is defined by ice sheet properties only, $\langle S\rangle - S_0 = a/(\beta c)$. This glaciation extent may be reduced by ocean damping factor $(\alpha+\kappa/c)\gamma_1/\gamma_3$ or enhanced by ocean positive feedback $(\alpha+\kappa/c)\gamma_2/\gamma_3$.

We will measure the total ocean impact Ω as a difference between the strength of ocean positive feedback and damping factor:

$$\Omega = \left(\alpha + \frac{\kappa}{c}\right)\frac{\gamma_2}{\gamma_3} - \frac{1}{S_0}\left(\alpha + \frac{\kappa}{c}\right)\frac{\gamma_1}{\gamma_3}$$

and introduce a dimensionless number V (variability number) as a ratio of the intensity of ocean impact Ω to the intensity of ice sheet own negative feedback:

$$V = \frac{\Omega}{\beta} = \frac{\left(\alpha + \frac{\kappa}{c}\right)\left(\frac{\gamma_2}{\gamma_3} - \frac{1}{S_0}\frac{\gamma_1}{\gamma_3}\right)}{\beta} \tag{33}$$

This number is small if the oceanic positive feedback is weak and it is high otherwise. We will now demonstrate that the variability number V defines different modes of glacial rhythmicity.

Earth Syst. Dynam. Discuss., https://doi.org/10.5194/esd-2018-14
Manuscript under review for journal Earth Syst. Dynam.
Discussion started: 23 March 2018

Earth System Dynamics Discussions
Open Access
EGU

4.2 Mode I: Late Pleistocene. V=0.75

We will now present results of dynamical system evolution for the same set of parameters as in 4.1 but ε=0.1 km/ky. Very similar results have been produced for other sets of parameters as long as V=0.75+/-0.02, for example, α=2.1 and κ=0.006 km/ky/^{o}C (slightly increased ocean positive feedback), or β=1.8 ^{o}C/(10^6 km^2) (slightly decreased negative feedback), or γ_2 and γ_3 are proportionally increased by about 10%, or κ and c are proportionally increased by about 10%, and so on. On Fig. 3 we show results of calculations of the glaciation extent for the last 1,000,000 years together with LR04 benthic foraminifera δ^{18}O stack (Lisiecki and Raymo, 2005).

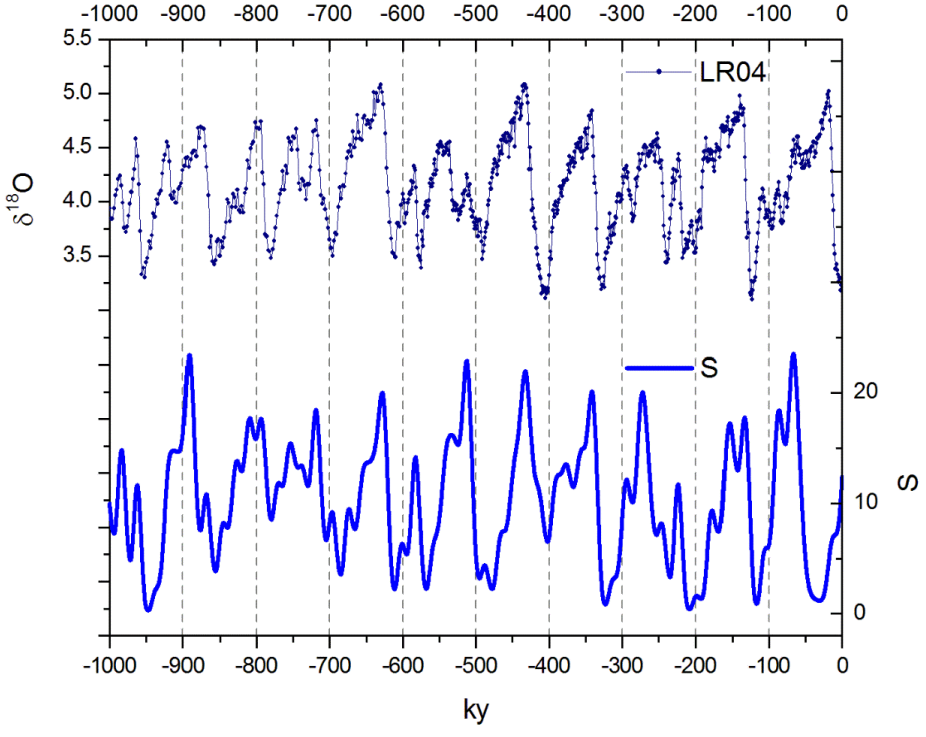

Fig. 3. Glacial rhythmicity over the past 1,000,000 years: Lisiecki and Raymo (2005) benthic foraminifera δ^{18}O data (**top**); System (24) - (26) produced evolution of glaciation area S (10^6 km^2) (**bottom)**.

Earth Syst. Dynam. Discuss., https://doi.org/10.5194/esd-2018-14
Manuscript under review for journal Earth Syst. Dynam.
Discussion started: 23 March 2018

The major events of the last million years are reproduced reasonably well, except, for the interglacial of 400 ky ago (marine isotopic stage 11), which has usually been described as a long and deep interglacial, and, obviously, the last interglacial starting 30,000 years ago instead of 10,000 years ago, and driving the present-day into a glaciation. The timing of all other interglacials coincides with Past Interglacial Working Group of PAGES (2016) data. Some tuning efforts at this point could be exercised to get even better fit, but we believe that exact replication should not be expected from a simple model like ours taking into account all uncertainties involved in parameters values. It should also be recalled that benthic curve is not strictly a measure of only ice volume.

Fig. 4 compares the modeled ocean temperature ω with the reconstruction of tropical ocean temperatures provided by Herbert et al (2010).

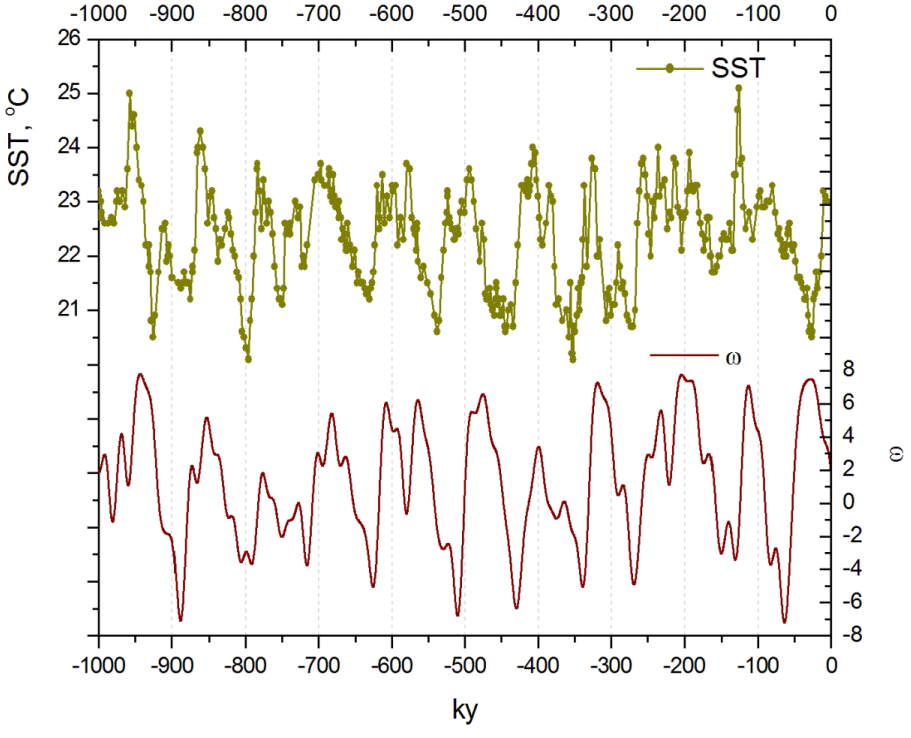

Fig. 4. Ocean temperature evolution over the past 1,000,000 years: Herbert *et al* (2010) data of tropical ocean temperatures (**top**); System (24) - (26) produced evolution of ocean temperature changes ω (^{o}C) (**bottom)**.

It can be noted that calculated temperature changes and ocean temperature data generally evolve in phase, though, like in the case with glaciation extent (Fig.3), last interglacial slightly leads data.

Earth Syst. Dynam. Discuss., https://doi.org/10.5194/esd-2018-14
Manuscript under review for journal Earth Syst. Dynam.
Discussion started: 23 March 2018

On Fig. 5 we compare spectral diagrams for calculated glaciation volume ($\zeta S^{5/4}$) against LR04 benthic $\delta^{18}O$ data and for calculated ω values against Herbert et al (2010) tropical ocean temperatures data. In both cases, results are reasonably consistent: In all cases periods near-100 ky clearly dominate. Precession and obliquity periods can be easily distinguished, though in both empirical diagrams 40-ky periods are more visible than in the model.

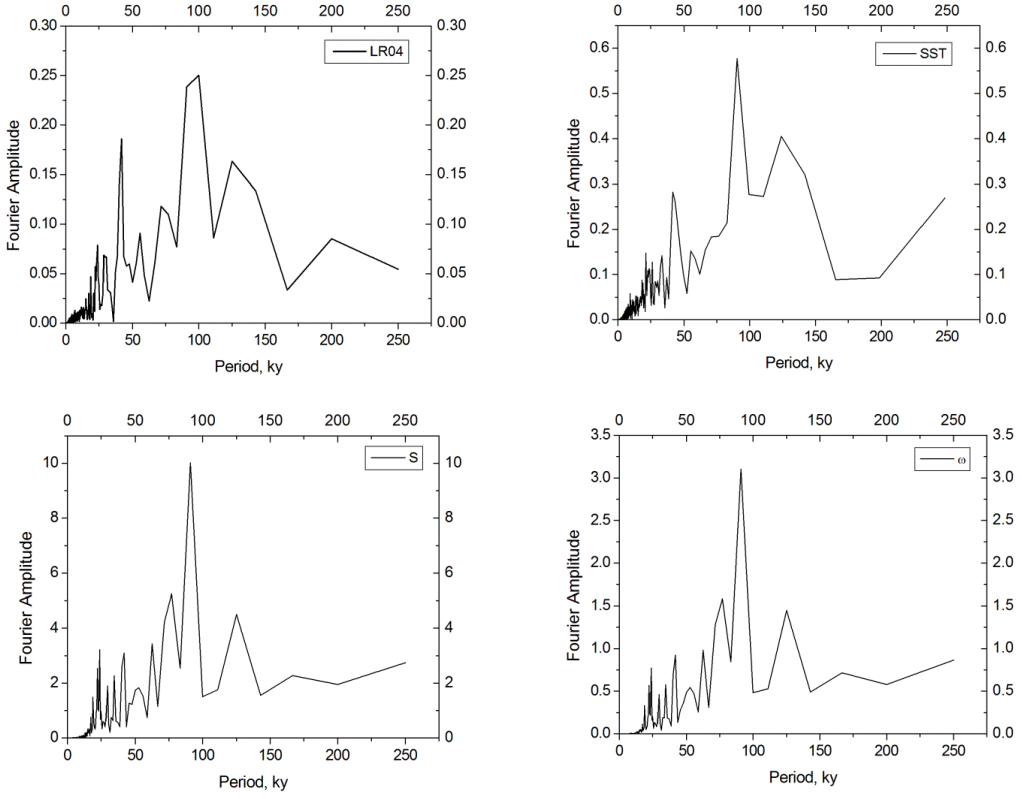

Fig. 5. Spectral diagrams of LR04 benthic foraminifera $\delta^{18}O$ data (**left top**), calculated glaciation volume,$\zeta S^{5/4}$ (**left bottom**), Herbert et al (2010) tropical ocean temperatures data (**right top**), and calculated ω values (**right bottom**).

The sequence of events which produce 100-ky periods can be visualized by zooming into a typical cycle. For this purpose, in Fig. 6, we show the evolution of the derivatives of the model variables, together with insolation changes.

Earth Syst. Dynam. Discuss., https://doi.org/10.5194/esd-2018-14
Manuscript under review for journal Earth Syst. Dynam.
Discussion started: 23 March 2018

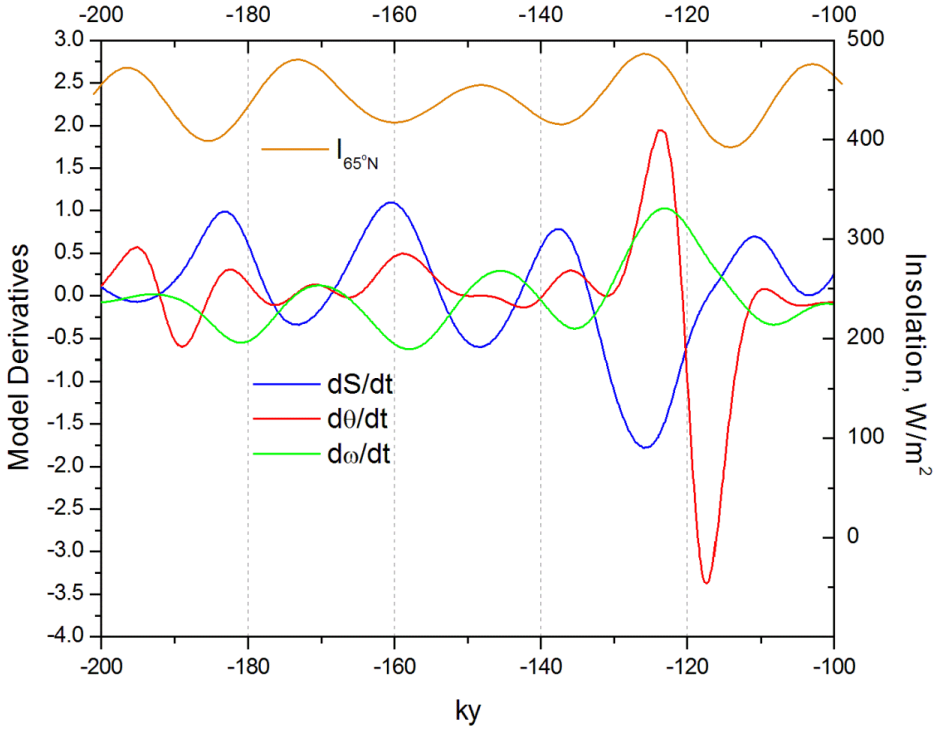

Fig. 6. Time evolution of model derivatives during one glacial cycle against insolation chages.

It can be seen that when ice grows, its basal temperature increases (with a time lag) due to increased internal friction and due to a more prominent role of the geothermal heat flux. As we discussed earlier, it provides a negative feedback to ice sheet growth. At the same time, ocean temperature is getting lower as well, and it creates a positive feedback for ice growth. Four times during this cycle the astronomical force "challenges" ice growth trying to switch it to the disintegration mode. These attempts fail three times: Ice volume is not high enough and positive feedback from the ocean acting through its mass balance ($\kappa\omega$) and through basal temperature ($\alpha\omega$) is not strong enough to counteract ice sheet own negative feedback (βS). The fourth attempt succeeds. Ice is high enough, positive feedback is strong, and disintegration proceeds until ice almost disappears. This scenario is consistent with the idea that glacial cycles skip insolation cycles until ice has grown to a point that precipitates its full disintegration, as conceptualized among others by Paillard (1998) and Tzedakis et al.(2017). It is to some extent reminiscent to the phase locking mechanism mathematically analyzed by Tziperman, et al. (2006) and Crucifix (2013). In our model,

Earth Syst. Dynam. Discuss., https://doi.org/10.5194/esd-2018-14
Manuscript under review for journal Earth Syst. Dynam.
Discussion started: 23 March 2018

Earth System Dynamics
Discussions
Open Access
EGU

though, the role of insolation is much bigger than in phase-locking scenarios: Insolation variations define not only the phase of ice fluctuations but, being non-linearly amplified, they actually define the period of glacial rhythmicity as well. The mechanism involved in the glacial frequency setting is similar to a "period-two" (period doubling) response to astronomical forcing exhibited by a conceptual model of Daruka and Ditlevsen (2016). To illustrate this "period-two" behavior, we solve our system (24) - (26) with astronomical forcing replaced by a single obliquity-period sinusoid $F_S=\varepsilon\ sin(2\pi t/41ky)$. The results of calculations, presented on Fig. 7, show that for relatively high amplitude of forcing (ε >0.07) our model produces fluctuations of a doubled obliquity period.

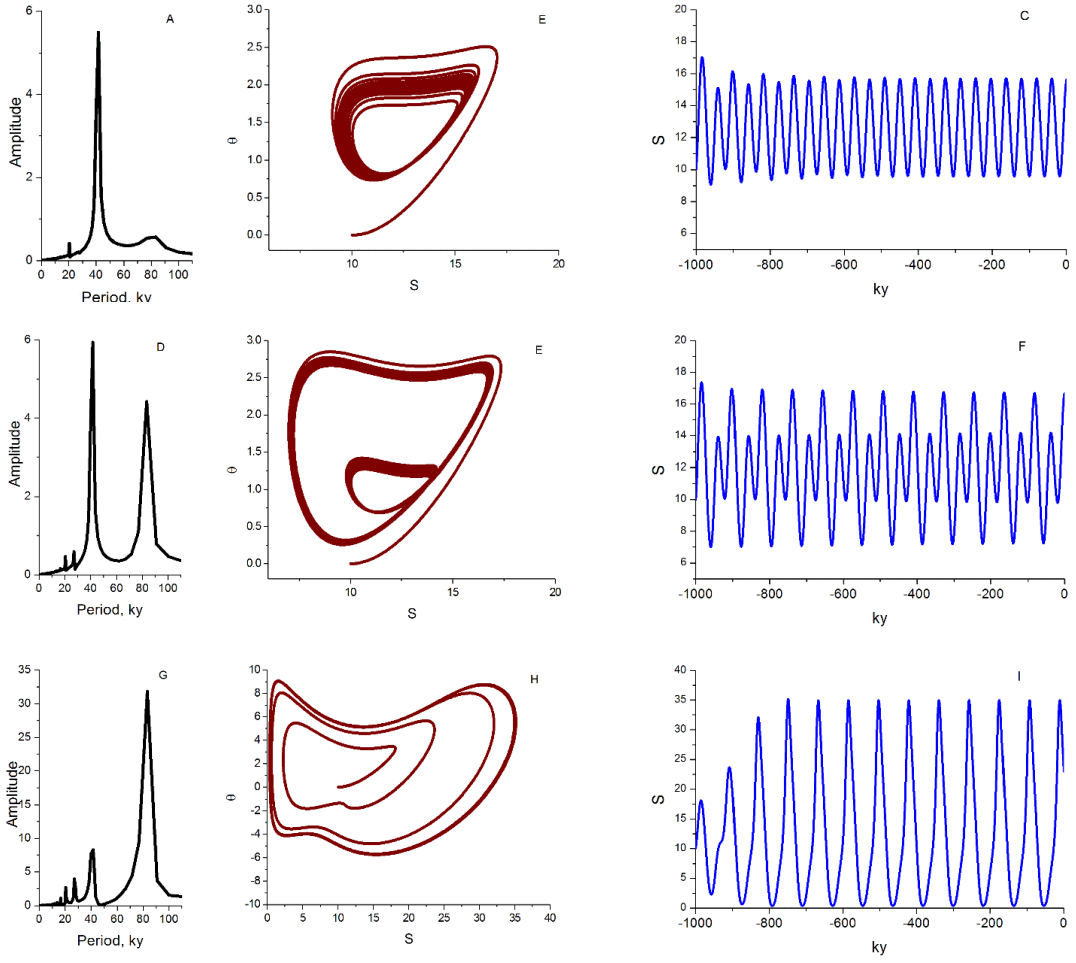

Fig. 7. Model response to a single obliquity-period sinusoid $F_S=\varepsilon\ sin(2\pi t/41ky)$. Subplots (A,B,C): ε=0.07; (D,E,F): ε=0.082; (G,H,I): ε=0.11. Subplots (A,D,G) are Fourier spectra; (B,E,H) are phase diagrams, S (10^6 km^2) *vs.* θ ^{o}C;

Earth Syst. Dynam. Discuss., https://doi.org/10.5194/esd-2018-14
Manuscript under review for journal Earth Syst. Dynam.
Discussion started: 23 March 2018

(C,F,I) are time series, S (10^6 km^2). For V=0.75 and relatively high amplitude of forcing (ε >0.07) model (24) - (26) produces fluctuations of a doubled obliquity period.

Until full dynamical system analysis is performed, which is clearly outside of the scope of this paper, we will (loosely) reference this mechanism as "non-linear amplification" and we will demonstrate that this mechanism manifests itself differently depending on V-number which is a measure of positive-to-negative feedback ratio.

4.3 Mode II: Late Pliocene/early Pleistocene. V=0.

We will now present results of dynamical system evolution for the same set of parameters as in 4.2 but α=0 and κ=0 (or $\gamma_2 = \gamma_1$=0), i.e., ocean feedback is weak, V=0. Results of calculations are shown in Fig.8.

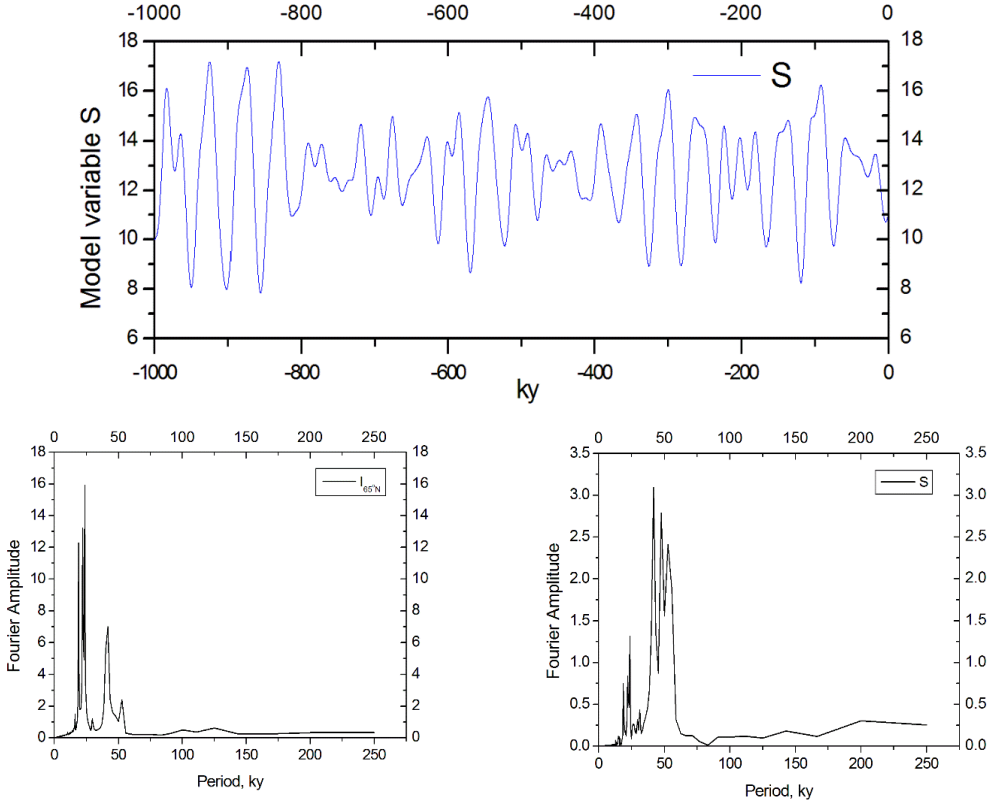

Fig. 8. Example of variable S (10^6 km^2) evolution for Mode II (**top**). Spectral diagrams of summer insolation changes at 65°N (**left bottom**) and of calculated glaciation volume, $\zeta S^{5/4}$ (**right bottom**)

Earth Syst. Dynam. Discuss., https://doi.org/10.5194/esd-2018-14
Manuscript under review for journal Earth Syst. Dynam.
Discussion started: 23 March 2018

The local mid-July insolation at 65°N, F_S, (Berger and Loutre, 1991) is dominated by precession period of about 23 ky (Fig. 8, left bottom), while the early Pleistocene paleoclimatic data speak about stronger response in the 40-ky period band. The integrated summer insolation, which is dominated by the 41 kyr obliquity cycle (Huybers, 2006), is often invoked to explain this discrepancy. It is interesting that our model produces fluctuations with dominating obliquity period (Fig. 8 , right bottom) without needing integrated summer forcing. It happens due to period-doubling dynamics, but in this case, on precession periods. To illustrate this phenomenon, we solve our system (24) - (26) with astronomical forcing replaced by a single precession-period sinusoid $F_S=\varepsilon\ sin(2\pi t/23ky)$. The results of calculations, presented on Fig. 9, show that when V=0 our model produces fluctuations of a doubled precession period.

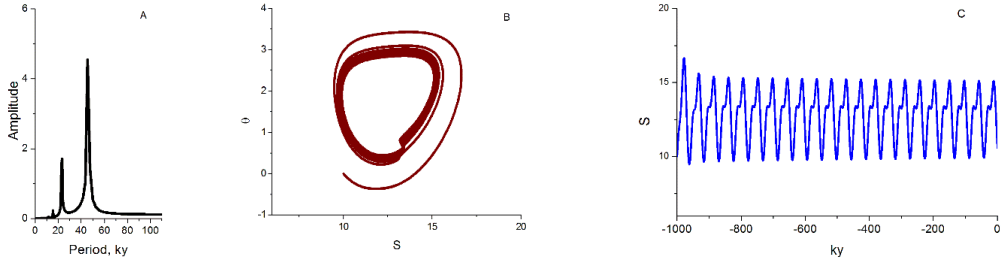

Fig. 9. Model response to a single precession-period sinusoid $F_S=\varepsilon\ sin(2\pi t/23ky)$: For V=0 and ε=0.04 model (24) - (26) produces fluctuations of a doubled precession period. Subplot A: Fourier spectra; Subplot B: Phase diagram, S (10^6 km^2) *vs.* θ °C; Subplot C: Time series, S (10^6 km^2).

If we also set S_0=2 (10^6 km^2) we will get fluctuations with lower mean level of ice area extension which may be relevant to early Pleistocene fluctuations (Fig. 10).

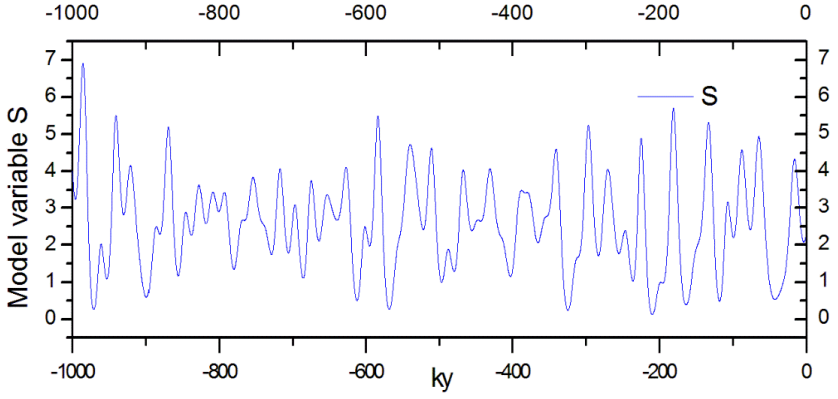

Earth Syst. Dynam. Discuss., https://doi.org/10.5194/esd-2018-14
Manuscript under review for journal Earth Syst. Dynam.
Discussion started: 23 March 2018

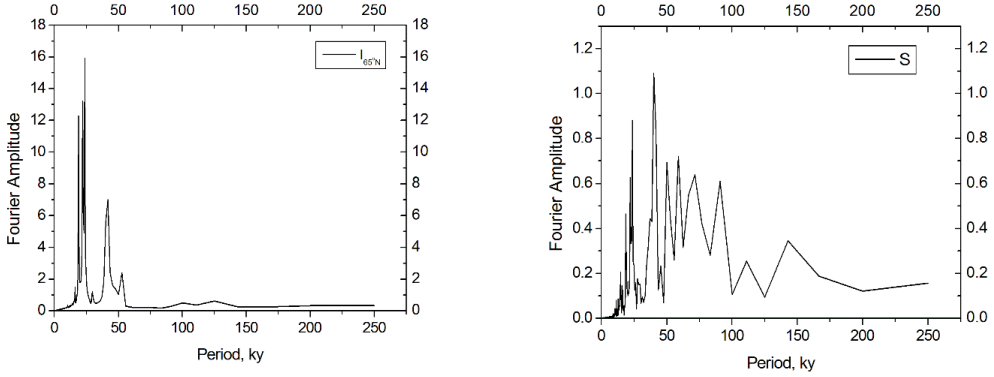

Fig. 10. Example of variable S (10^6 km^2) evolution for Mode II (**top**). S_0=2 (10^6 km^2). Spectral diagrams of summer insolation changes at 65°N (**left bottom**) and of calculated glaciation volume,$\zeta S^{5/4}$ (**right bottom**)

Astronomical periods are still very visible in ice spectral diagram of ice fluctuations.

4.4 Mode III: Strong ocean feedback : $V \rightarrow 1$.

In this section we show that the system would produce fluctuations of about 400 ky if the ocean positive feedback increased further ($V \rightarrow 1$). Specifically, we present results of dynamical system evolution for the same set of parameters as in 4.2 but β=1.57 °C/(10^6 km^2), i.e., V=0.94. Very similar results have been produced for different sets of parameters as long as $V \sim 0.95$, for example γ_2=0.26 °C/(10^6 km^2)/ky.

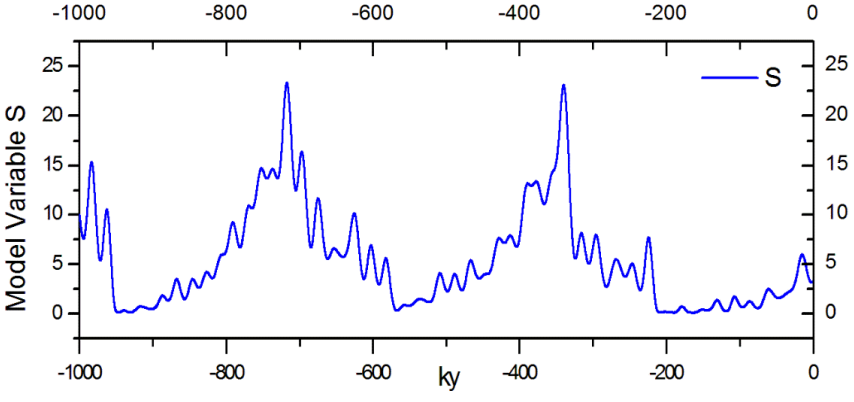

Fig. 11. Example of variable S (10^6 km^2) evolution for Mode III.

The results may seem to be counterintuitive at first because one would expect faster ice growth as the positive feedback increases. However, it makes sense by observing that with stronger positive feedback every astronomical "challenge" is more successful in retreating ice. Consequently, it takes longer to grow ice to the level where its retreat can be really strong. The ratio between positive and negative feedbacks determines how long it takes for ice

Earth Syst. Dynam. Discuss., https://doi.org/10.5194/esd-2018-14
Manuscript under review for journal Earth Syst. Dynam.
Discussion started: 23 March 2018

to grow until a level at which it is vulnerable to the astronomical "challenge" (in our model it corresponds roughly to S~ 20x10^6 km^2). This example also shows that if the ratio between positive and negative feedbacks were wrong (i.e., wrong V-number) then the astronomical forcing would in no case reproduce the correct sequence of events. In other words, incorrect physics cannot be rescued by tuning the strength of the astronomical forcing.

4.5 Mode II - Mode I Transition (Mid-Pleisctocene Transition)

If we attribute V=0 mode to early Pleistocene and V=0.75 mode to late Pleistocene, then the V-number may provide some guidance about scenarios possible to explain mid-Pleistocene transition. Since the V-number is a combination of multiple parameters, it implies that multiple scenarios are possible. For memory, $V=(1/\beta)(\alpha+\kappa/c)(\gamma_2/\gamma_3 - \gamma_1/\gamma_3/S_0)$, where the parameters β, c, and S_0 are glaciation parameters, α and κ are parameters associated with atmospheric circulations, and γ_1, γ_2, and γ_3 are ocean parameters. We think it is less likely that β and c parameters were be involved in the transition scenarios because, for the most part, ice sheet thermodynamics must have remained the same. However, forced variations of atmospheric, or ocean, or both groups of parameters are quite possible. It is outside of the scope of this paper to provide a full list of scenarios possible, but at least one plausible suggestion can be made. A commonly invoked scenario involves tectonic forcing, including volcanism and weathering processes which could produced long-term variations of carbon dioxide such that it dropped from above 300 ppm during the early Pliostocene to its current values of about 250 ppm. The scenario remains commonly invoked (Saltzman and Maasch, 1991; Saltzman and Verbitsky, 1993a,b; Raymo 1997; Paillard and Parrenin, 2004) even though it is fair to admit that the observations remain uncertain (Zhang et al, 2013) and that this scenario has been challenged (Honish *et al*, 2009). Whether or not this specific mechanism is responsible for the regime change, it still seems reasonable to assume that the slow trend in climatic condition occurred and that it can cause a drift in the ocean positive feedback (γ_2), specifically, an increase from lower to higher values. As an illustration, in Figs. 12-14 we present an example of such transition. In this instance, at t=-3,000 ky, γ_2, S_0, and ε have been reduced by 60% from their Mode I values and then increased linearly, so that they regained 100% of their Mode I values at present (t=0). Forced change of the glaciation reference line S_0 defines gradual increase of the global ice volume; changes of the sensitivity parameter ε cause increase of fluctuations' amplitude. The most dramatic change, i.e., transition from about 40-ky-period fluctuations to predominantly 100-ky-period fluctuations is due to the intensified ocean positive feedback , γ_2, which caused gradual increase of V-number from V=0.3 at t=-3,000 ky to V=0.75 at present (t=0). The example shows reasonable consistency between model results and the data: In model calculations and in the records of instrumental measurements (Fig. 13), early Pleistocene is dominated by mostly 40-ky fluctuations. At about 1.5 - 1.3 My ago, 100-ky rhythmicity becomes predominant. Its amplitude is at a maximum about 400 ky ago in both instrumental and model time series. The evolution of cross-wavelet spectrum (Grinsted *et al*, 2004) between benthic foraminifera δ^{18}O data and system (24) - (26) produced evolution of glaciation area S (Fig. 14) shows mostly in-phase relationship between model and measurements' records on 40 ky and 100 ky periods.

Earth Syst. Dynam. Discuss., https://doi.org/10.5194/esd-2018-14
Manuscript under review for journal Earth Syst. Dynam.
Discussion started: 23 March 2018

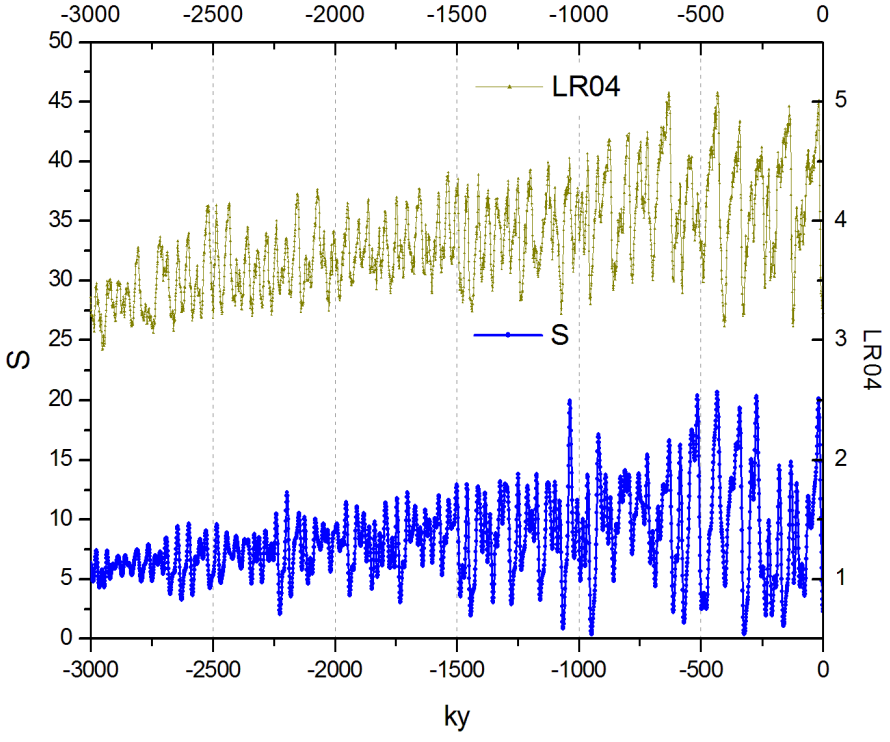

Fig. 12. Glacial rhythmicity over the past 3,000,000 years: Lisiecki and Raymo (2005) benthic foraminifera $\delta^{18}O$ data (**top**); System (24) - (26) produced evolution of glaciation area S (10^6 km^2) (**bottom**).

Earth Syst. Dynam. Discuss., https://doi.org/10.5194/esd-2018-14
Manuscript under review for journal Earth Syst. Dynam.
Discussion started: 23 March 2018

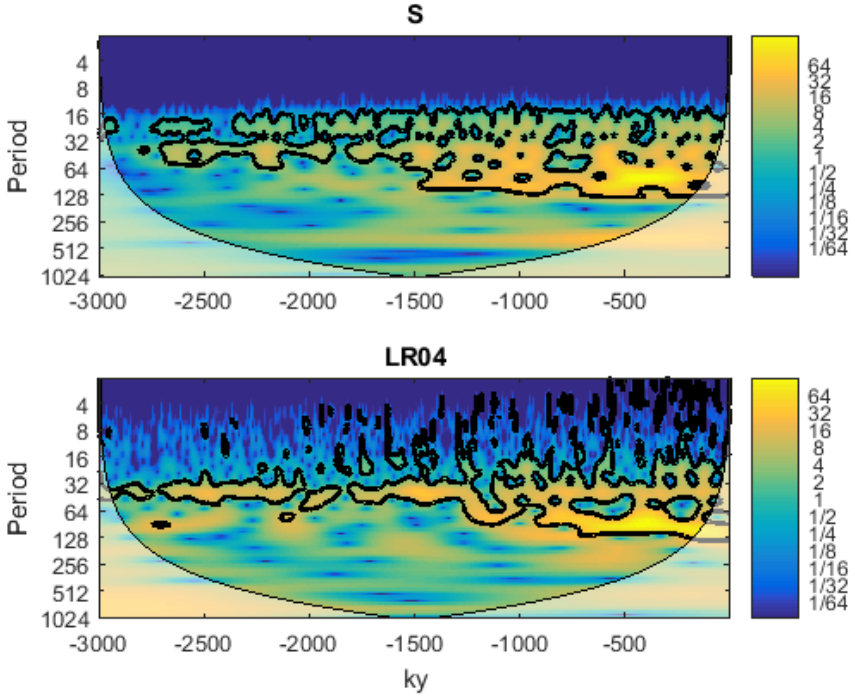

Fig. 13. Evolution of wavelet spectra over the past 3,000,000 years. System (24) - (26) produced evolution of glaciation area S (10^6 km^2) (**top);** Lisiecki and Raymo (2005) LR04 benthic foraminifera $\delta^{18}O$ data (**bottom**). Color scale shows wavelet amplitude, thick line bounds the peaks with 95% confidence, shaded area indicates the cone of influence for wavelet transform.

Earth Syst. Dynam. Discuss., https://doi.org/10.5194/esd-2018-14
Manuscript under review for journal Earth Syst. Dynam.
Discussion started: 23 March 2018

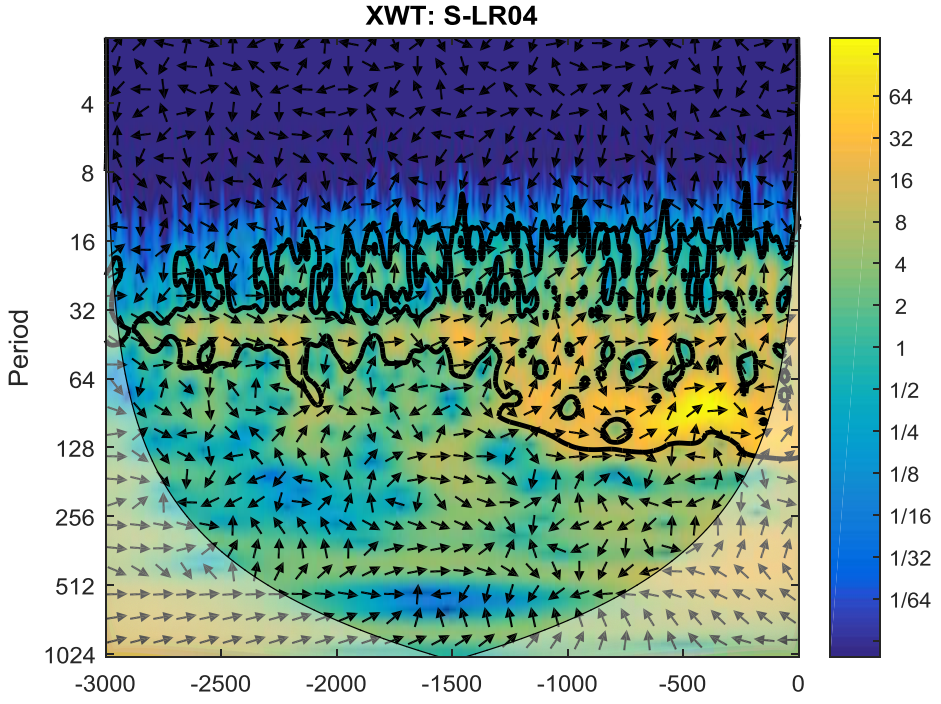

Fig. 14. Evolution of cross-wavelet spectrum (Grinsted *et al*, 2004) between Lisiecki and Raymo (2005) benthic foraminifera $\delta^{18}O$ data and system (24) - (26) produced evolution of glaciation area *S***.** Higher cross-wavelet power (color bar scale) shows areas with high common power wavelet spectra, thick contour shows 95% significance of maxima against red noise. The phase relationship is shown with arrows, where "in-phase" relation is indicated by arrows directed to the right and "anti-phase"- by arrows directed to the left.

Earth Syst. Dynam. Discuss., https://doi.org/10.5194/esd-2018-14
Manuscript under review for journal Earth Syst. Dynam.
Discussion started: 23 March 2018

Earth System Dynamics Discussions Open Access EGU

4.6 Role of the Antarctic ice sheet.

System (24) - (26) can be expanded to include the Southern Hemisphere (Antarctic) ice dynamics:

$$\begin{cases} \dfrac{dS}{dt} = \dfrac{4}{5}\zeta^{-1}S^{3/4}(a - \varepsilon F_S - \kappa\omega - c\theta) & (34) \\ \dfrac{d\theta}{dt} = \zeta^{-1}S^{-1/4}(a - \varepsilon F_S - \kappa\omega)\{\alpha\omega + \beta[S - S_o] - \theta\} & (35) \\ \dfrac{d\omega}{dt} = \gamma_1 - \gamma_2[S - S_o + S_A - S_A^{\max}] - \gamma_3\omega & (36) \\ \dfrac{dS_A}{dt} = \dfrac{4}{5}\zeta^{-1}S_A{}^{3/4}(a_A - \varepsilon F_{SA} - \kappa\omega - c_A\theta_A); S_A \le S_A^{\max} & (37) \\ \dfrac{d\theta_A}{dt} = \zeta^{-1}S_A{}^{-1/4}(a_A - \varepsilon F_{SA} - \kappa\omega)\{\alpha\omega + \beta[S_A - S_o] - \theta_A\} & (38) \end{cases}$$

Here equations (34) and (35) are identical to equations (24) and (25). Equations (37) and (38) describe the evolution of the glaciation area of the Antarctic ice sheet S_A and its basal temperature θ_A; F_{SA} is mid-January insolation at 65°S (Berger and Loutre, 1991); S_A^{max} is the area of the Antarctic continent; a_A is rate of snow precipitation and c_A is intensity of basal sliding for Antarctic ice sheet. All other parameters in (37), (38) are intentionally left the same as in (35) and (36), following the assumption that Antarctic ice sheet and Northern Hemisphere ice sheets are governed by the same physics. Equation (36) is the same as (26) except that it includes an additional term to reflect a potential control by Antarctic ice sheet and associated ice shelves ($-\gamma_2[S_A - S_A^{max}]$). The system (34) - (38) is represented graphically in Fig.15.

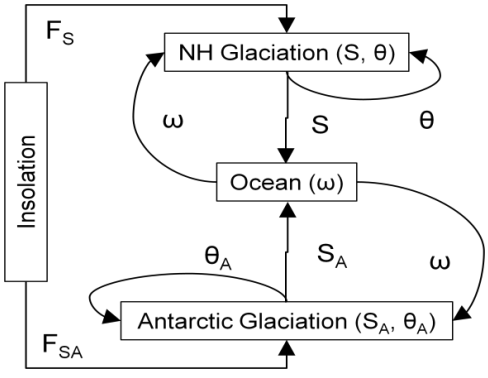

Fig. 15. Global dynamical climate system (34) - (38).

Earth Syst. Dynam. Discuss., https://doi.org/10.5194/esd-2018-14
Manuscript under review for journal Earth Syst. Dynam.
Discussion started: 23 March 2018

Earth System Dynamics Discussions Open Access EGU

System (34) - (38) has been solved for the same set of parameters as in 4.1 but a_A=0.5km/ky and c_A=0.01 km/ky/^{o}C (implying more positive mass balance of the Antarctic ice sheet than the one of Northern Hemisphere ice sheets). For this set of parameters $S_A = S_A^{max}$ =const and system (34) - (38) takes the following shape:

$$\begin{cases} \dfrac{dS}{dt} = \dfrac{4}{5}\zeta^{-1}S^{3/4}(a - \varepsilon F_S - \kappa\omega - c\theta) & (39) \\ \dfrac{d\theta}{dt} = \zeta^{-1}S^{-1/4}(a - \varepsilon F_S - \kappa\omega)\{\alpha\omega + \beta[S - S_o] - \theta\} & (40) \\ \dfrac{d\omega}{dt} = \gamma_1 - \gamma_2[S - S_o] - \gamma_3\omega & (41) \\ S_A = S_A^{\max} & (42) \\ \dfrac{d\theta_A}{dt} = \zeta^{-1}S_A^{-1/4}(a_A - \varepsilon F_{SA} - \kappa\omega)\{\alpha\omega + \beta[S_A^{\max} - S_o] - \theta_A\} & (43) \end{cases}$$

Now, equations (39) - (41) are exactly the same as in our original system (24) - (26). It means that all previous calculations were conducted with the assumption that area of Antarctic glaciation remains constant. Interestingly, the system (39) - (43) has a "diode"-like structure (Fig. 16): Northern Hemisphere insolation has important impact on Northern Hemisphere glaciation, the extent of glaciation effects ocean temperature, ocean temperature effects Antarctic climate and eventually ice sheet basal temperature

$$F_S \rightarrow S \rightarrow \omega \rightarrow \alpha\omega \text{ and } \kappa\omega \rightarrow \theta_A,$$

but since $S_A = S_A^{max}$ =const, there is no "opportunity" for Southern Hemisphere insolation to be amplified by ocean positive feedback and to propagate its signal north.

Earth Syst. Dynam. Discuss., https://doi.org/10.5194/esd-2018-14
Manuscript under review for journal Earth Syst. Dynam.
Discussion started: 23 March 2018

Earth System Dynamics
Discussions
Open Access
EGU

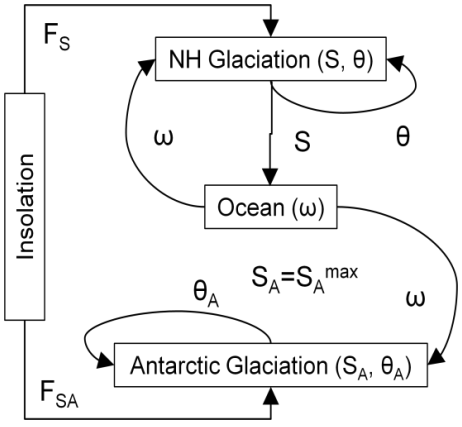

Fig. 16. Global dynamical climate system (34) - (38) in the "diode"-like mode: $S_A = S_A^{max}$ =const.

This produces a simple explanation to the synchronous response of the Northern and Southern Hemispheres to Northern Hemisphere insolation variations.

5. Conclusions

In this research, we build the theory of Pleistocene ice ages without a prior assumption about internal climate system instability. For this purpose, we derived a simple model of the global climate system using scaled equations of ice sheet thermodynamics, to combine them with a linear equation describing changes of ocean temperature. The model obtained is a non-linear dynamical system incorporating three variables: area of glaciation, ice sheet basal temperature, and ocean temperature. Without astronomical forcing, the system evolves to equilibrium. When it is astronomically forced, then, depending on the values of parameters involved, the system is capable of producing different modes of rhythmicity, some of which are consistent with paleoclimate records of early and late Pleistocene.

Three mechanisms captured by our model are of primary importance. The first one is a nonlinear dependence of the intensity of ice discharge on ice sheet dimensions: $dS/dt \sim S^{3/4}$. This non-linearity was postulated by Huybers (2009) as being proportional to ice volume in 9-th degree; here we were able to quantify it using fundamentals of ice flow revealed by equation (5). The second mechanism is basal sliding intensity. Its importance was expressed by MacAyeal (1993), Payne (1995) and by Marshall and Clark (2002) for the Laurentide ice sheet. In this paper, using scaling of ice thermodynamics, we were able to connect sliding intensity to climatic factors. When internal ice sheet dynamics are coupled with the rest of the climate system via a linear ocean equation, the above two phenomena, jointly, form a third one - the non-linear amplification of the insolation forcing. This amplification defines not only the phase but also the period of glacial rhythmicity by producing multi-obliquity and multi-precession periods similar to a conceptual model of Daruka and Ditlevsen (2016). We determined that this mechanism manifests itself differently depending on a specific balance between positive and negative feedbacks in the system.

To measure this balance, we introduced a dimensionless variability number or *V*-number as the ratio between intensities of glaciation and ocean feedbacks. When the ocean positive feedback is weak ($V \sim 0$), the system exhibits fluctuations with dominating period of about 40 ky which is in fact a combination of doubled precession period and (to smaller extent) obliquity period. When the ocean positive feedback increases ($V \sim 0.75$), the system evolves with a roughly 100-ky period which is a doubled obliquity period. Finally, when the ocean positive feedback increases

further (V~0.95), the system produces fluctuations of about 400 ky. When the V-number is gradually increased from its low early Pleistocene values to its late Pleistocene value of V=0.75, the system reproduces the mid-Pleistocene transition: While early Pleistocene is dominated by mostly 40-ky fluctuations, at about 1.5 My ago the 100-ky-period rhythmicity emerges and finally dominates.

Thus, our theory is capable of explaining all major features of the Pleistocene climate benthic isotopic record, including the mostly 40-ky fluctuations of the early Pleistocene, a transition from a 40-ky-non-linear regime to a 100-ky-non-linear regime, and the 100-ky fluctuations of the late Pleistocene.

The crucial role of ocean feedback is evident in the Southern Hemisphere as well. Antarctic ice sheet area of glaciation is limited by the Antarctic continent and therefore it cannot engage a strong positive feedback from the ocean. At the same time, the impact of the Northern Hemisphere is amplified by the ocean and affects the Antarctic climate. This may provide an explanation of the synchronous response of the Northern and Southern Hemispheres to Northern Hemisphere insolation variations.

The system we described in this paper has eleven (11) parameters, but all of them are at least partly constrained. Some of them are based on empirical data of present ice sheets and others can be calibrated with a three-dimensional ice sheet model and global general circulation climate models. Most revealing though, as we discussed above, is the V-number, a dimensionless combination of eight (8) parameters. Given that V-number is dimensionless, this model could be used to investigate other physics which may be involved in producing ice ages. In such a case, the equation currently representing ocean temperature would describe some other climate component of interest, like the marine or terrestrial carbon cycle, dust transport, *etc*. As long as this component is capable of producing an appropriate V-number, it may be considered as an acceptable candidate. However, we have not found it necessary to assume a priori a non-linearity in the equations governing ocean or carbon cycle dynamics to explain ice age cycles as they appear in the benthic isotopic record.

Authors' contribution: MV conceived the research and developed the model. MV, MC, and DV contributed equally to the design of the research and to writing the manuscript. DV digitized the model.

Competing interests: The authors declare no competing financial interests.

Acknowledgement:

We are grateful to David Pollard for providing results of numerical experiments with a three-dimensional Antarctic ice-sheet model and inspiring discussions.

Earth Syst. Dynam. Discuss., https://doi.org/10.5194/esd-2018-14
Manuscript under review for journal Earth Syst. Dynam.
Discussion started: 23 March 2018

Earth System Dynamics Discussions
Open Access
EGU

Appendix: Calibration of the scaling model with 3-D model of the Antarctic Ice Sheet[1]

To test the response of ice-sheet basal temperature to climatic factors such as precipitation rate, air temperature, and ice-sheet area, four numerical experiments have been conducted with a 3-D ice-sheet model applied to Antarctica:

A. Current climate: ***da/a*=0, *dT*=0, *dS/S*=0**
B. Increased (doubled) precipitation: ***da/a*=1, *dT*=0, *dS/S*=0**
C. Increased temperature (with unavoidable retreat of the ice sheet): ***da/a*=0, *dT*=10C, *dS/S*= -0.38**
D. Increased precipitation and increased temperature: ***da/a*=1, *dT*=10C, *dS/S*= -0.29**

The ice sheet-shelf model used here is described in detail in Pollard and DeConto (2012a) and additionally in Pollard et al. (2015) and DeConto and Pollard (2016). It uses a hybrid combination of Shallow Ice Approximation and Shallow Shelf Approximation (SIA-SSA) dynamics, which consider vertical shearing (SIA) and horizontal stretching (SSA) while neglecting higher-order modes of flow. A flux condition at the grounding line (Schoof, 2007) is imposed that allows reasonable grounding line migration without very fine resolution in the grounding zone. These approximations yield satisfactory results in long-term large-scale intercomparisons vs. higher-order models (Pattyn et al., 2012, 2013). The distribution of basal sliding coefficients under modern grounded regions is determined from a previous inverse run fitting to modern ice thicknesses (Pollard and DeConto, 2012b). There is no explicit basal hydrology; basal sliding is allowed only if the base is at or close to the melt point. All experiments here are run on a polar stereographic grid with 20 km grid resolution.

Atmospheric climate forcing is obtained from a modern Antarctic climatological dataset (ALBMAP; Le Brocq et al., 2010). Monthly mean air temperatures and precipitation are interpolated to the ice-sheet grid and lapse-rate corrected to the ice surface elevation (Pollard and DeConto, 2012a), and a simple model is used to estimate net surface mass balance using Positive-Degree-Day melting and refreezing. Oceanic melting below floating ice shelves depends on the 400-m water temperature at the nearest grid cell in a modern oceanographic dataset (Levitus et al., 2012).

The experiments are initialized to the modern Antarctic state (Bedmap2; Fretwell et al., 2013). All experiments are run with invariant climate forcing for 100,000 years to ensure that the ice sheet is very nearly equilibrated. The standard physical ice sheet model is used, except that grounding-line locations and ice shelf distributions are held fixed to modern (as in Pollard and DeConto, 2012b), to avoid grounding-line advance in marine sectors that would complicate interpretation of the results. For experiment A (current climate control), modern climate forcing is used as described above. For experiment B, prescribed precipitation rates are doubled everywhere. For experiment C, a uniform increment of +10 ^{o}C is added to all prescribed atmospheric temperatures. For experiment D, the modifications for B and C are combined. In all experiments, the lapse-rate adjustment to precipitation rates is disabled, to ensure that precipitation rates in experiments B and D are exactly double those in A and C.

The results of the experiments are shown on Figs. A1-A3 where we show basal temperature changes relative to the present climate. Table A1 presents integrated results.

[1]The Appendix has been provided by David Pollard.

Earth Syst. Dynam. Discuss., https://doi.org/10.5194/esd-2018-14
Manuscript under review for journal Earth Syst. Dynam.
Discussion started: 23 March 2018

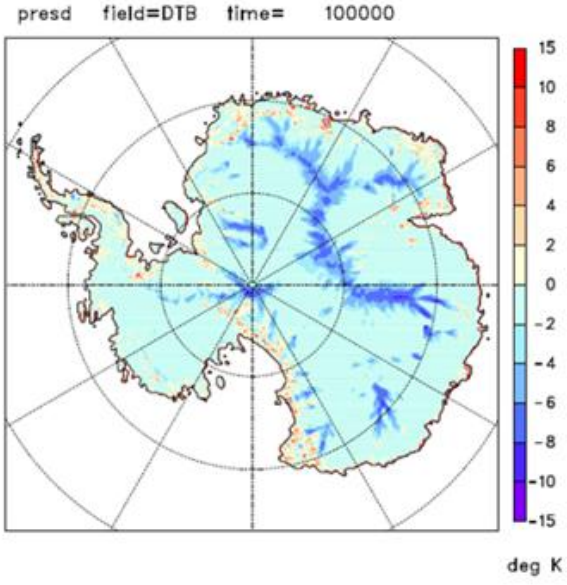

Fig. A1. Basal ice temperature change for experiment B minus the control experiment A. These are absolute temperature changes, not relative to the pressure melt point.

Earth Syst. Dynam. Discuss., https://doi.org/10.5194/esd-2018-14
Manuscript under review for journal Earth Syst. Dynam.
Discussion started: 23 March 2018

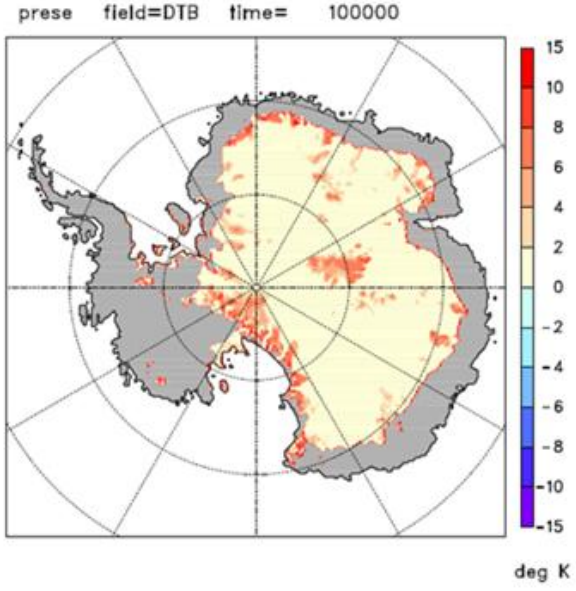

Fig. A2. Basal ice temperature change for experiment C minus the control experiment A (absolute temperature changes, not relative to the pressure melt point).

Earth Syst. Dynam. Discuss., https://doi.org/10.5194/esd-2018-14
Manuscript under review for journal Earth Syst. Dynam.
Discussion started: 23 March 2018

Earth System Dynamics Discussions Open Access EGU

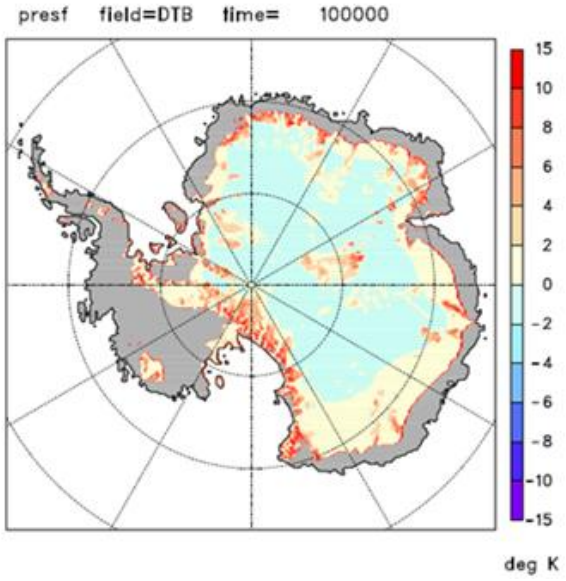

Fig. A3. Basal ice temperature change for experiment D minus the control experiment A (absolute temperature changes, not relative to the pressure melt point).

Table A1. Basal temperature changes relative to the present climate (^{o}C)

B $\left[\frac{da}{a}=1; dT=0; \frac{dS}{S}=0\right]$		**C** $\left[\frac{da}{a}=0; dT=10C; \frac{dS}{S}=-0.38\right]$		**D** $\left[\frac{da}{a}=1; dT=10C; \frac{dS}{S}=-0.29\right]$	
Equations (14)-(16)	3-D experiment	Equations (14)-(16)	3-D experiment	Equations (14)-(16)	3-D experiment
-5.7	-2.0	9.6	3.7	4.0	3.0

As seen in Table A1, the sign and order of magnitude of the basal temperature response to climatic forcing predicted by our scaling estimates are consistent with the results of the 3-D ice-sheet model.

References

Abe-Ouchi A., F. Saito, K. Kawamura, M. E. Raymo, J. I. Okuno, K. Takahashi and H. Blatter (2013). Insolation-driven 100,000-year glacial cycles and hysteresis of ice-sheet volume, Nature, (500) 190--193 doi:10.1038/nature12374

Ashkenazy, Y., & Tziperman, E. (2004). Are the 41kyr glacial oscillations a linear response to Milankovitch forcing?. Quaternary Science Reviews, 23(18), 1879-1890.

Ashwin P. and P. Ditlevsen (2015). The middle Pleistocene transition as a generic bifurcation on a slow manifold, Climate Dynamics, 45 (9–10) 2683–2695 doi:10.1007/s00382-015-2501-9

Berger, A., Loutre, M. F. (1991). Insolation values for the climate of the last 10 million years. Quaternary Science Reviews, 10(4), 297-317.

Chalikov, D. V., and Verbitsky, M. Y. (1990). Modeling the Pleistocene ice ages. Advances in Geophysics 32, 75-131

Clark P. U., D. Archer, D. Pollard, J. D. Blum, J. A. Rial, V. Brovkin, A. C. Mix, N. G. Pisias and M. Roy (2006). The middle Pleistocene transition: characteristics. mechanisms, and implications for long-term changes in atmospheric PCO_2, Quat. Sci. Rev., (25) 3150-3184 doi:10.1016/j.quascirev.2006.07.008

Crucifix M. (2013). Why could ice ages be unpredictable? Clim Past, vol. 9 (5) pp. 2253-2267. doi:10.5194/cp-9-2253-2013

Crucifix, M., Rougier, J. (2009). On the use of simple dynamical systems for climate predictions. The European Physical Journal-Special Topics, 174(1), 11-31

Daruka I. and P. D. Ditlevsen (2016). A conceptual model for glacial cycles and the middle Pleistocene transition, Climate Dynamics, (46) 29–40 doi:10.1007/s00382-015-2564-7

DeConto, R.M., and D. Pollard (2016). Contribution of Antarctica to past and future sea-level rise. Nature, 531, 591-597.

Ellis, R., & Palmer, M. (2016). Modulation of ice ages via precession and dust-albedo feedbacks. Geoscience Frontiers, 7(6), 891-909.

Fretwell, P., H.D. Pritchard, D.G. Vaughan, J.L. Bamber, N.E. Barrand, R. Bell, C. Bianchi, R.G. Bingham, D.D. Blankenship, G. Casassa, G. Catania, D. Callens, H. Conway, A.J. Cook, H.F.J. Corr, D. Damaske, V. Damm, F. Ferraccioli, R. Forsberg, S. Fujita, Y. Gim, P. Gogineni, J.A. Griggs, R.C.A. Hindmarsh, P. Holmlund, J.W. Holt, R.W. Jacobel, A. Jenkins, W. Jokat, T. Jordan, E.C. King, J. Kohler, W. Krabill, M. Riger-Kusk, K.A. Langley, G. Leitchenkov, C. Leuschen, B.P. Luyendyk, K. Matsuoka, J. Mouginot, F.O. Nitsche, Y. Nogi, O.A. Nost, S.V. Popov, E. Rignot, D.M. Rippin, A. Rivera, J. Roberts, N. Ross, M.J. Siegert, A.M. Smith, D. Steinhge, M. Studinger, B. Sun, B.K. Tinto, B. C. Welch, D. Wilson, D. Young, C. Xiangbin, and A. Zirizzotti (2013). Bedmap2: improved ice bed, surface and thickness datasets for Antarctica. The Cryo., 7, 375-393.

Ganopolski A. and D. M. Roche (2009). On the nature of lead--lag relationships during glacial--interglacial climate transitions, Quaternary Science Reviews, (28) 3361--3378 doi:10.1016/j.quascirev.2009.09.019

Ganopolski A., R. Calov, and M. Claussen (2010). Simulation of the last glacial cycle with a coupled climate ice-sheet model of intermediate complexity, Climate of the Past, (6) 229--244 doi:10.5194/cp-6-229-2010

Grinsted, Aslak, John C. Moore, and Svetlana Jevrejeva (2004). Application of the cross wavelet transform and wavelet coherence to geophysical time series. Nonlinear processes in geophysics 11.5/6: 561-566.

Herbert, T. D., Peterson, L. C., Lawrence, K. T., & Liu, Z. (2010). Tropical ocean temperatures over the past 3.5 million years. Science, 328(5985), 1530-1534.

Honisch B., N. G. Hemming, D. Archer, M. Siddall and J. F. McManus (2009). Atmospheric Carbon Dioxide Concentration Across the Mid-Pleistocene Transition, Science, (324) 1551–1554 doi:10.1126/science.1171477

Huybers, P. (2006). Early Pleistocene glacial cycles and the integrated summer insolation forcing. Science, 313(5786), 508-511.

Huybers, P. (2009). Pleistocene glacial variability as a chaotic response to obliquity forcing. Climate of the Past, 5(3), 481-488.

Imbrie, J. Z., Imbrie-Moore, A., and Lisiecki, L. E. (2011). A phase-space model for Pleistocene ice volume, Earth and Planetary Science Letters, 307, 94-102.

Le Brocq, A.M., A.J. Payne, and A. Vieli (2010). An improved Antarctic dataset for high resolution numerical ice sheet models (ALBMAP v1). Earth Sys. Sci. Data, 2, 247-260.

Levitus, S., J.I. Antonov, T.P. Boyer, O.K. Baranova, H.E. Garcia, R.A. Locarnini, A.V. Mishonov, J.R. Reagan, D. Seidov, E.S. Yarosh, and M.M. Zweng (2012). World ocean heat content and thermosteric sea level change (0-2000 m), 1955-2010. Geophys. Res. Lett., 39, L10603, doi:10.1029/2012GL051106.

Lisiecki, L. E., Raymo, M. E. (2005). A Pliocene-Pleistocene stack of 57 globally distributed benthic $\delta^{18}O$ records. Paleoceanography, 20(1).

MacAyeal, D. R. (1993). Binge/purge oscillations of the Laurentide ice sheet as a cause of the North Atlantic's Heinrich events. Paleoceanography, 8(6), 775-784.

Marshall, S. J., Clark, P. U. (2002). Basal temperature evolution of North American ice sheets and implications for the 100kyr cycle. Geophysical Research Letters, 29(24).

Mitsui, T., Aihara, K. (2014). Dynamics between order and chaos in conceptual models of glacial cycles. Climate dynamics, 42(11-12), 3087-3099.

Omta A. W., B. W. Kooi, G. A. K. Voorn, R. E. M. Rickaby and M. J. Follows (2016). Inherent characteristics of sawtooth cycles can explain different glacial periodicities, Climate Dynamics, (46) 557–569 doi:10.1007/s00382-015-2598-x

Paillard D. (1998). The timing of Pleistocene glaciations from a simple multiple-state climate model, Nature, (391) 378-381 doi:10.1038/34891

Paillard, D. (2015). Quaternary glaciations: from observations to theories, Quaternary Science Reviews, (107) 11--24 doi:http://dx.doi.org/10.1016/j.quascirev.2014.10.002

Paillard, D., Parrenin, F. (2004). The Antarctic ice sheet and the triggering of deglaciations. Earth and Planetary Science Letters, 227(3), 263-271.

Past Interglacial Working Group of PAGES (2016). Interglacials of the last 800,000 years. Rev. Geophys. 54, 162–219.

Paterson, W. S. B. (1981). The physics of glaciers, Oxford: Pergamon Press.

Pattyn, F., C. Schoof, L. Perichon, R.C.A. Hindmarsh, E. Bueler, B. de Fleurian, G. Durand, O. Gagliardini, R. Gladstone, D. Goldberg, G.H. Gudmundsson, P. Huybrechts, V. Lee, F. M. Nick, A.J. Payne, D. Pollard, O. Rybak, F. Saito, and A. Vieli (2012). Results of the Marine Ice Sheet Model Intercomparison Project, MISMIP. The Cryo., 6, 573-588.

Pattyn, F. L. Perichon, G. Durand, L. Favier, O. Gagliardini, R.C.A. Hindmarsh, T. Zwinger, T. Albrecht, S. Cornford, D. Docquier, J.J. Fürst, D. Goldberg, G.H. Gudmundsson, A. Humbert, M. Hütten, P. Huybrechts, G. Jouvet, T. Kleiner, E. Larour, D. Martin, M. Morlighem, A.J. Payne, D. Pollard, M. Rückamp, O. Rybak, H. Seroussi, M. Thoma, and N. Wilkens (2013). Grounding-line migration in plan-view marine ice-sheet models: results of the *ice2sea* MISMIP3d intercomparison. J. Glaciol., 59, 410-422.

Payne, A. J. (1995). Limit cycles in the basal thermal regime of ice sheets. Journal of Geophysical Research: Solid Earth, 100(B3), 4249-4263.

Pollard, D., and R.M. DeConto (2012a). Description of a hybrid ice sheet-shelf model, and application to Antarctica. Geosci. Model Devel., 5, 1273-1295.

Pollard, D., and R.M. DeConto (2012b). A simple inverse method for the distribution of basal sliding coefficients under ice sheets, applied to Antarctica. The Cryosphere, 6, 953-971.

Pollard, D., R.M. DeConto, and R.B. Alley (2015). Potential Antarctic Ice Sheet retreat driven by hydrofracturing and ice cliff failure. Earth Plan. Sci. Lett., 412, 112-121.

Raymo M. (1997), The timing of major climate terminations, Paleoceanography, (12) 577-585 doi:10.1029/97PA01169

Ruddiman W. F. (2006), Ice-driven CO_2 feedback on ice volume, Climate of the Past, (2) 43-55 doi:10.5194/cp-2-43-2006

Saltzman, B. (2002). Dynamical paleoclimatology: generalized theory of global climate change (Vol. 80). Academic Press.

Saltzman, B., Maasch, K. A. (1991). A first-order global model of late Cenozoic climatic change II. Further analysis based on a simplification of CO 2 dynamics. Climate Dynamics, 5(4), 201-210.

Saltzman, B., Verbitsky, M. Y. (1992). Asthenospheric ice-load effects in a global dynamical-system model of the Pleistocene climate. Climate Dynamics, 8(1), 1-11.

Saltzman, B., Verbitsky, M. Y. (1993a). Multiple instabilities and modes of glacial rhythmicity in the Plio-Pleistocene: a general theory of late Cenozoic climatic change. Climate Dynamics, 9(1), 1-15.

Saltzman, B., Verbitsky, M. Y. (1993b). The late Cenozoic glacial regimes as a combined response to earth-orbital variations and forced and free CO_2 variations. In Ice in the Climate System. Edited by W.R. Peltier (pp. 343-361). Springer, Berlin, Heidelberg.

Saltzman, B., Verbitsky, M. (1994a). Late Pleistocene climatic trajectory in the phase space of global ice, ocean state, and CO_2: Observations and theory. Paleoceanography, 9(6), 767-779.

Saltzman, B., Verbitsky, M. (1994b). CO_2 and glacial cycles. Nature, 367(6462), 419-419.

Schoof, C. (2007), Ice sheet grounding line dynamics: steady states, stability, and hysteresis. J. Geophys. Res.-Earth Surf.112, F03S28.

Shumskiy, P. A. (1975). On the flow law for polycrystalline ice. Trudy instituta mekhaniki MGU, 42, 54-68.

Tzedakis P. C., M. Crucifix, T. Mitsui and E. W. Wolff (2017), A simple rule to determine which insolation cycles lead to interglacials, Nature, (542) 427–432 doi:10.1038/nature21364

Tziperman, E., Raymo, M. E., Huybers, P., & Wunsch, C. (2006). Consequences of pacing the Pleistocene 100 kyr ice ages by nonlinear phase locking to Milankovitch forcing. Paleoceanography, 21(4).

Verbitsky, M., Chalikov, D. V. (1986). Modelirovaniye Sistemy Ledniki-Okean-Atmosfera.[Modelling of the Glaciers-Ocean-Atmosphere System]. Gidrometeoizdat.

Vialov, S. S. (1958). Regularities of glacial shields movement and the theory of plastic viscous flow. Physics of the movements of ice IAHS, 47, 266-275.

Zhang Y. G., M. Pagani, Z. Liu, S. M. Bohaty and R. DeConto (2013), A 40-million-year history of atmospheric CO_2, Philosophical Transactions of the Royal Society A: Mathematical, Physical and Engineering Sciences, (371) 20130096–20130096 doi:10.1098/rsta.2013.0096